

Article

The Multi-Objective Optimization of Low-Impact Development Facilities in Shallow Mountainous Areas Using Genetic Algorithms

Huiyi Sun ¹, Yuxiang Dong ², Yue Lai ¹ , Xuanyin Li ¹, Xiaoyu Ge ^{1,*}  and Chensong Lin ^{1,*}¹ School of Landscape Architecture, Beijing Forestry University, Beijing 100000, China² College of Architecture and Urban Planning, Tongji University, Shanghai 200092, China

* Correspondence: gexiaoyu@bjfu.edu.cn (X.G.); linchensong@bjfu.edu.cn (C.L.); Tel.: +86-13811819956 (C.L.)

Abstract: From the perspective of whole-area sponge city construction, it is important to scientifically determine the layout plan of LID facilities for controlling urban rainfall and flooding problems, given the topographical features and rainfall runoff characteristics of shallow urban mountainous areas. Current research on the optimization of low-impact development facilities is limited to the central urban area level, with insufficient research on shallow urban mountainous areas, and there is great uncertainty in the layout of LID facilities when multiple objectives are considered. Therefore, this paper applied a genetic algorithm (NSGA-II) to optimize the layout scheme of LID facilities. Multiple objectives of the peak runoff abatement rate, cost, and land area were selected as the optimization objectives, and the optimized results were ranked using the EWM-TOPSIS and VCWM-TOPSIS methods. The 2nd Hebei Provincial Garden Flower Expo (Qinhuangdao) Park was used as the research object for the optimization design. The results showed that, under the premise of water safety, the lowest cost priority was given to the LID facility with a 15.49% share, 99.43% peak runoff reduction rate, and a cost of CNY 1.215×10^7 ; the lowest area priority was given to the LID facility with a 15.25% share, 99.42% peak runoff reduction rate, and a cost of CNY 1.267×10^7 . The EWM-TOPSIS method was also used to obtain the best optimized solution with 16.18% LID facilities, 99.64% peak runoff abatement rate, and a cost of CNY 1.26×10^7 , and the worst optimized solution with 12.55% LID facilities, 97.91% peak runoff abatement rate, and a cost of CNY 1.061×10^7 . The decision results under different decision-maker preferences were obtained by the VCWM-TOPSIS method. This study showed that the combination of a genetic algorithm and TOPSIS can optimize the layout of LID facilities in shallow mountainous areas more scientifically and efficiently compared to the actual construction plan for building a sponge city.

Keywords: stormwater management models; shallow mountain areas; cost; low-impact development; genetic algorithms



Citation: Sun, H.; Dong, Y.; Lai, Y.; Li, X.; Ge, X.; Lin, C. The Multi-Objective Optimization of Low-Impact Development Facilities in Shallow Mountainous Areas Using Genetic Algorithms. *Water* **2022**, *14*, 2986. <https://doi.org/10.3390/w14192986>

Academic Editor: Richard C. Smardon

Received: 19 August 2022

Accepted: 19 September 2022

Published: 23 September 2022

Publisher's Note: MDPI stays neutral with regard to jurisdictional claims in published maps and institutional affiliations.



Copyright: © 2022 by the authors. Licensee MDPI, Basel, Switzerland. This article is an open access article distributed under the terms and conditions of the Creative Commons Attribution (CC BY) license (<https://creativecommons.org/licenses/by/4.0/>).

1. Introduction

Over-urbanization has increased the impermeable area of cities and rising surface runoff, leading to frequent urban flooding. To cope with urban flooding, China has proposed the concept of a “sponge city,” and at present, the construction of sponge cities in China has achieved certain results. However, due to the pilot policy implemented in China, the construction of sponge cities is divided into key areas, so the key areas in a city have the function of a sponge city after construction [1]. However, from a city-wide perspective, the construction of sponge cities presents a relatively independent situation without systematic construction [2]. Therefore, in April 2021, the Ministry of Housing and Urban-Rural Development first put forward the “Notice on Carrying Out Systematic Territory-wide Demonstration of Sponge City Construction”, and China launched two batches of territory-wide sponge city construction demonstration cities in 2021 and

2022, with a total investment amount of approximately CNY 44.8 billion, as well as a large number of construction projects [3]. Therefore, promoting territory-wide sponge city construction is of top priority. The construction of region-wide sponge cities needs to be tailored to the local conditions of the region, especially in China, where the terrain is complex and diverse, the mountainous areas are vast, and the shallow mountainous areas, as transition zones between urban and mountainous areas, are an ecological barrier against mountainous runoff entering cities and natural boundary surfaces [4], so it is important to explore the construction of sponge cities in shallow mountainous areas.

The coupling of stormwater management models and intelligent computing can effectively simulate the effects of LID facilities in sponge cities and can quantify the simulation effects, which can facilitate the rational planning of LID facilities in sponge city construction [5–9].

Research on coupling stormwater management models (SWMMs) and genetic algorithms is popular at present [10,11]. Giacomoni et al. (2017) coupled a non-dominated sequencing genetic algorithm (NSGA-II) with a stormwater management model (SWMM) and applied it to an urban catchment to obtain the optimal location of the LID [12]. Hou et al. (2020) designed a stormwater treatment system and analyzed an integrated model that used a non-dominated sequencing genetic algorithm (NSGA-II) applied to a campus to obtain optimal spatial layout solution [13]. Huang et al. (2022) used a genetic algorithm (GA) to optimize LID selection and layout in the Tianjin economic zone [14]. Liu et al. (2021) used a non-dominated sequencing genetic algorithm (NSGA-II) to achieve automatic optimization of runoff control for infrastructure in the Wuhan Sponge City pilot region [15]. Although genetic algorithms have produced more results in optimizing LID facility layout solutions, most studies have focused on built-up urban areas or new development zones [16,17], and there is still a gap in the research in terms of shallow urban mountainous areas.

To fill this research gap, this paper proposes specific research objectives: (1) to validate the rainfall runoff model and simulate urban runoff in shallow mountainous areas through short-term rainfall events; (2) to couple the NSGA-II and SWMM models to optimize LID layout; (3) to rank options and comparisons with actual construction options using the EMW-TOPSIS and VCWM-TOPSIS methods; (4) to provide recommendations for the design of LID facilities in shallow urban mountainous areas. This study used the Qinhuangdao Economic and Technological Development Zone in Hebei Province as a case study to investigate how to deploy LID facilities in shallow urban mountainous areas to obtain the lowest cost, the least land use, and the best rainfall control solution. Three typical LID facilities—sunken green spaces, bioretention ponds, and rain gardens—were selected and developed, and multi-objective optimization was implemented.

2. Methodology

The entire research methodology included data collection, model calibration, runoff simulation, and LID optimization. Data collection included actual onsite measured water level data, geological survey report data, and the parameters required for the stormwater management model (SWMM). In addition, the site-measured flow production data were calibrated against the flow production data generated by the SWMM simulation, based on which the parameters were set to build a complete site model and runoff simulation was carried out by selecting the site sponge city construction standards. An optimization platform was built in the programming language Python, optimization objective functions were constructed, and the genetic algorithm NSGA-II was used to optimize the layout of LID facilities. The optimal LID solution was selected based on different preferences for peak runoff abatement rate, LID area, and cost, provided that the site meets the criteria for building a sponge city. Finally, the EWM-TOPSIS and VCWM-TOPSIS methods were applied to rank the options, and the option with the highest similarity was selected for comparison with the actual construction option. Figure 1 shows the detailed flow of the whole framework.

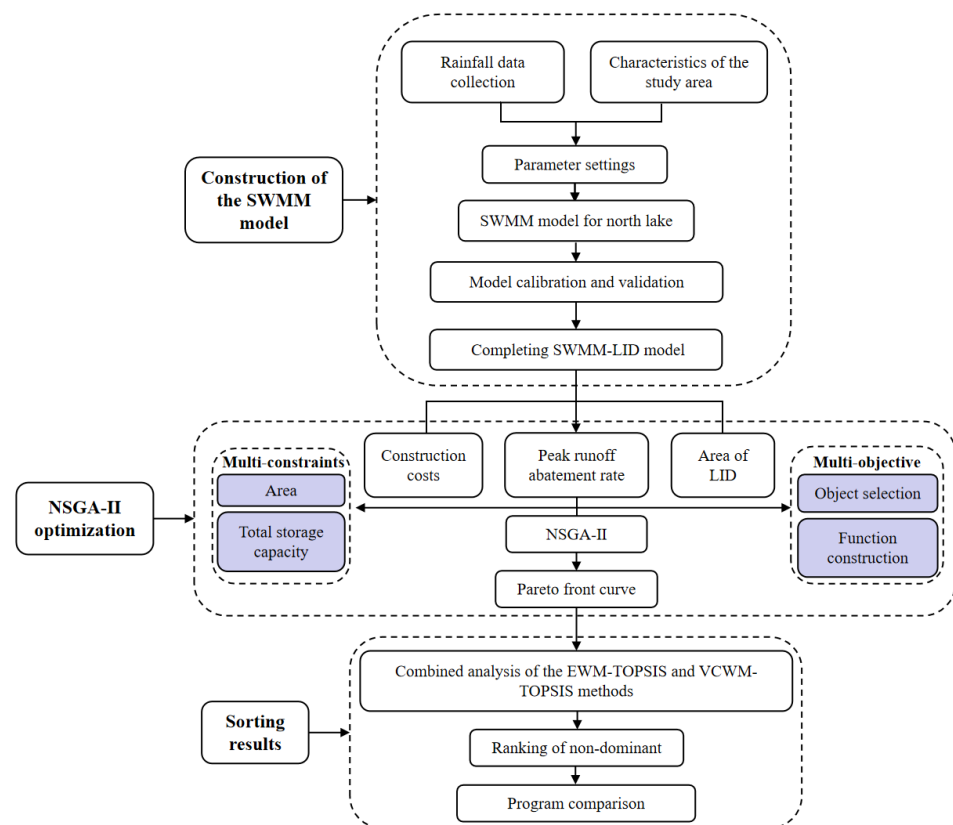


Figure 1. Flow chart of the research program.

2.1. Study Area

Qinhuangdao city is located on the main mountain range of the Qiyun Mountains. Here, most city regions are shallow mountainous areas, except for the built-up urban areas [18]. The study site is located at the junction of the Haigang and Beidaihe districts of Qinhuangdao city, Hebei Province (Figure 2a). It is located in the southeast of Qiyun Mountain, which has a relatively gentle slope range of 3–30° on the southeast side of the mountain (Figure 2b). The total site area is approximately 221.81 hm², of which 137.12 hm² comprises the 2nd Hebei Provincial Garden Flower Expo Park (hereinafter referred to as “the Expo Park”). The topography of Qiyun Mountains is fragmented, and the water catchment is mainly in the southeast direction. Runoff from the Qiyun Mountains joins the site along three existing washouts. It was calculated that the surrounding areas, such as the Qiyun Mountains and city roads, produce a catchment area of 101.64 hm² [19]. As a result, the site is under significant runoff pressure, and the eastern side of the Taifu Expressway and the city centre are under serious threat of rainwater flooding (Figure 2c). By sampling and testing the water at the site, the mean concentration of COD at the monitored site was calculated to be 12.45 mg/L.

Qinhuangdao city has a temperate continental monsoon climate with an extremely uneven distribution of rainfall seasons. The average annual precipitation is approximately 645.9 mm according to the weather station data across many years, and the annual precipitation is mainly concentrated in the summer, where the summer precipitation accounts for 69.7% of the annual average precipitation, with the maximum precipitation being able to reach 1038.5 mm [20]. The high intensity of rainfall in short calendar periods results in the problem of rainfall and flooding in shallow mountainous areas becoming even more acute. Therefore, the effective use of low-impact development facilities to regulate the site’s stormwater resources and attenuate surface runoff to solve the stormwater problems brought about by short duration and intense rainfall in the site and the city is an important measure to ensure site safety.

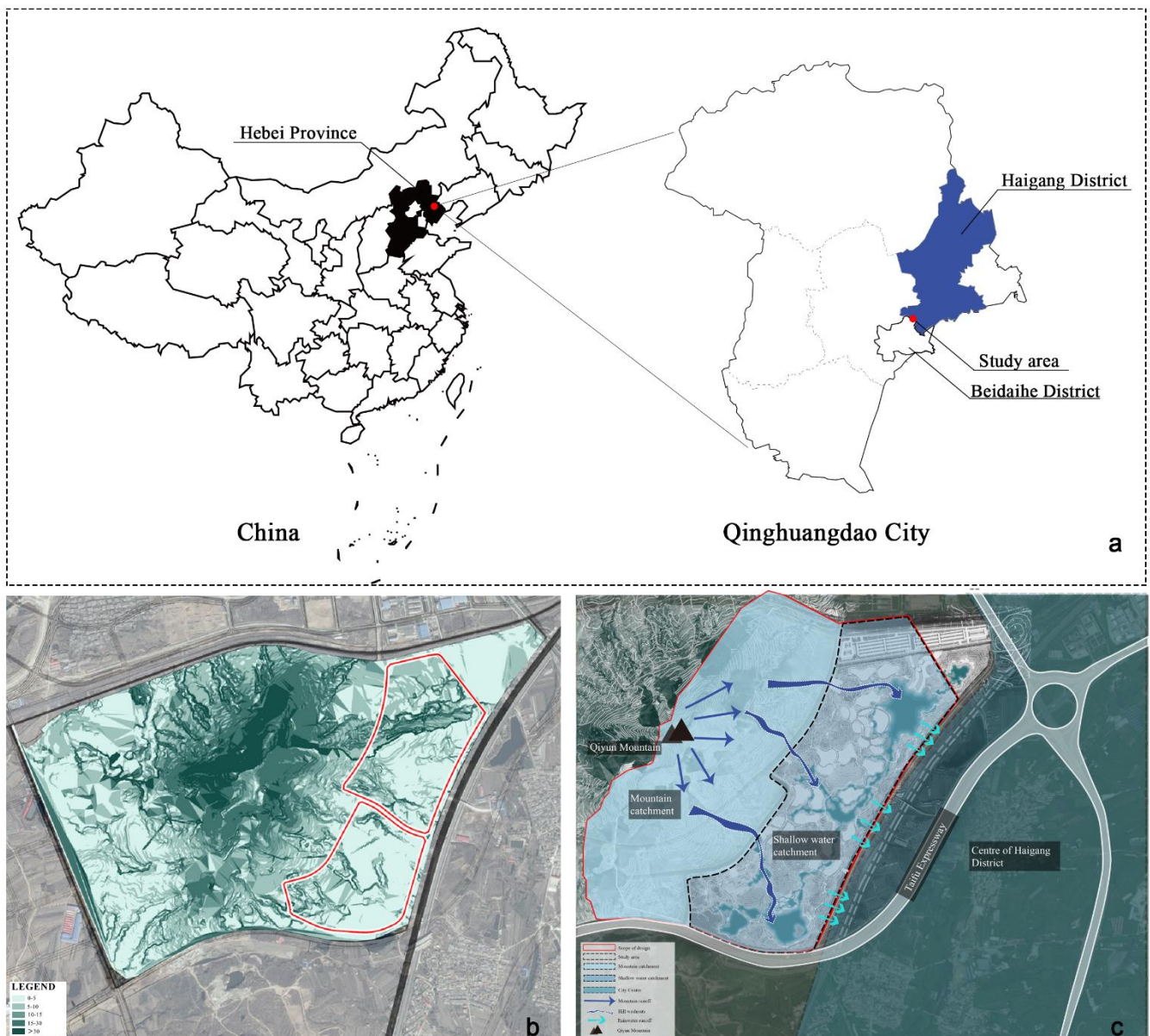


Figure 2. (a) Geographical location of the study area; (b) Slope of the study area; (c) Direction of water flow of the study area.

2.2. Rainfall Data

The rainfall data of 12 July 2021 were used for calibration, and the rainfall data of the recurrence period were used for the simulation. The rainfall data of the recurrence period were calculated according to the latest storm intensity formula of the Hebei Provincial Engineering Construction Standard “Engineering technical specification for construction of the sponge city” (DB13(J)/T 210-2016), and the storm intensity formula was [21]:

$$q = 605.709 \times (1 + 0.7111gP)/(t + 1.040)^{0.464} \quad (1)$$

where P is the design rainfall return period and t is the rainfall calendar time.

According to the “Standard for Design of Outdoor Wastewater Engineering” (GB50014-2021), the standard return period for flood control at the study site is 30 years, according to the classification to which Qinghuangdao city belongs [22]. Referring to the formula for the intensity of heavy rainfall in Qinghuangdao city, a 30-year rainfall event of 176.19 mm was calculated. Therefore, according to the Qinghuangdao Urban Drainage and Flood Control

Standard, this paper used this 30-year rainfall event (176.19 mm) as the standard to assess the effect of peak flow control of stormwater runoff.

2.3. Total Runoff Calculation

According to the “Technical code for urban flooding prevention and control” (GB51222-2017) and related specifications, when the peak flow rate is used as the control target, the total amount of runoff in the study site after optimizing the size of LID facilities after modification needs to be lower than the original total amount of runoff for the same design return period [23]. This is a prerequisite for assessing the effectiveness of stormwater control. According to the “Technical Guidelines for Sponge City Construction,” when total runoff control is used as the basis for design, the storage volume of the facility should generally meet the index requirements of “control volume per unit area.” The design storage volume is generally calculated using the volumetric method [24], with the formula for the volumetric method being:

$$V = 10H\varphi F \quad (2)$$

where V is the design storage volume in m^3 , H is the design rainfall in mm, φ is the integrated rainfall runoff coefficient, and F is the catchment area in hm^2 .

According to the study area, the 30-year rainfall $H = 176.19$ mm is selected, and the rainfall runoff coefficient is taken as φ , and the reference literature takes the value of $\varphi = 0.40$ [19], catchment area of the study area of $F = 221.81$ hm^2 , and a total runoff volume in the site of $156,322.82$ m^3 , as calculated by the formula. Therefore, the design total storage volume of the study area was $156,322.82$ m^3 , and the total storage volume of the site should be greater than or equal to $156,322.82$ m^3 after optimizing the layout plan of the LID facilities.

2.4. SWMM Simulation Verification

To verify the rainwater management model’s predictive capability, the rainfall data for 12 July 2021 were selected for model calibration. The rainfall on the site lasted for 24 h, amounting to 92.52 mm. The actual measurement onsite lasted for 2.5 h with a time interval of 15 min. The parameters of the rainwater management model (SWMM) were based on the internal engineering geological survey report of the site, the surface layer of the soil was vegetation fill and powder clay, and the weighted average of the two layers of soil had a thickness of approximately 2.1 m. According to the soil characteristics and the specification of “Planting Soil for Greening” (CJT340-2016), the HORTON infiltration model was selected [25]. The maximum infiltration rate was 80–360 mm/h, the saturation infiltration rate was 5–50 mm/h, the attenuation coefficient was 4 h^{-1} , and the other parameters were set according to the recommended values in the SWMM user manual and references [26,27]. The model parameters were adjusted by the trial-and-error method. After several trials and errors [28], a set of parameters reflecting the flow production of the site was obtained, as shown in Table 1.

Table 1. Regional rainfall runoff model parameter ranges.

| Model Parameters | Parameter Variation Range | |
|--|---------------------------|---------------|
| | Minimum Value | Maximum Value |
| width/m | 19 | 1909 |
| slope/% | 3 | 33.57 |
| N-Imperv | 0.012 | 0.012 |
| N-Perv | 0.8 | 0.8 |
| Dstore-Imperv | 1.27 | 1.27 |
| Dstore-Perv | 0.3 | 0.3 |
| Zero-Imperv/% | 100 | 100 |
| Initial infiltration/($\text{mm}\cdot\text{h}^{-1}$) | 80 | 360 |

Table 1. Cont.

| Model Parameters | Parameter Variation Range | |
|--|---------------------------|---------------|
| | Minimum Value | Maximum Value |
| Minimum infiltration/(mm·h ⁻¹) | 5 | 50 |
| Decay Constant/h | 4 | 4 |

The rainfall event at this site and its runoff data were selected for model calibration, and the results are shown in Figure 3. To verify the model, the quality of the calibration was assessed using three metrics: mean error (ME), mean absolute error (MAE), and root mean square error (RAMSE) [29,30]. The formula was calculated as follows:

$$\begin{aligned}
 ME &= \frac{1}{n} \sum_{i=1}^n (h_0 - h_c)_i \\
 MAE &= \frac{1}{n} \sum_{i=1}^n |(h_0 - h_c)_i| \\
 RMSE &= \left[\frac{1}{n} \sum_{i=1}^n (h_0 - h_c)_i^2 \right]^{0.5}
 \end{aligned} \quad (3)$$

In Equation (3), n denotes the number of real measurements, h_0 denotes the real tested yield flow value, and h_c denotes the simulated yield flow value.

The mean error (ME) was calculated to be -0.07 , the mean absolute error (MAE) was 0.07 , and the root mean square error (RMSE) was 0.1 . The results of the calculations indicate that the model's simulated and measured yield flow results are in good agreement. The set of parameters is a good reflection of the relationship between rainfall production at the site, and therefore, the model has a more credible runoff simulation capability and can be used for further research.

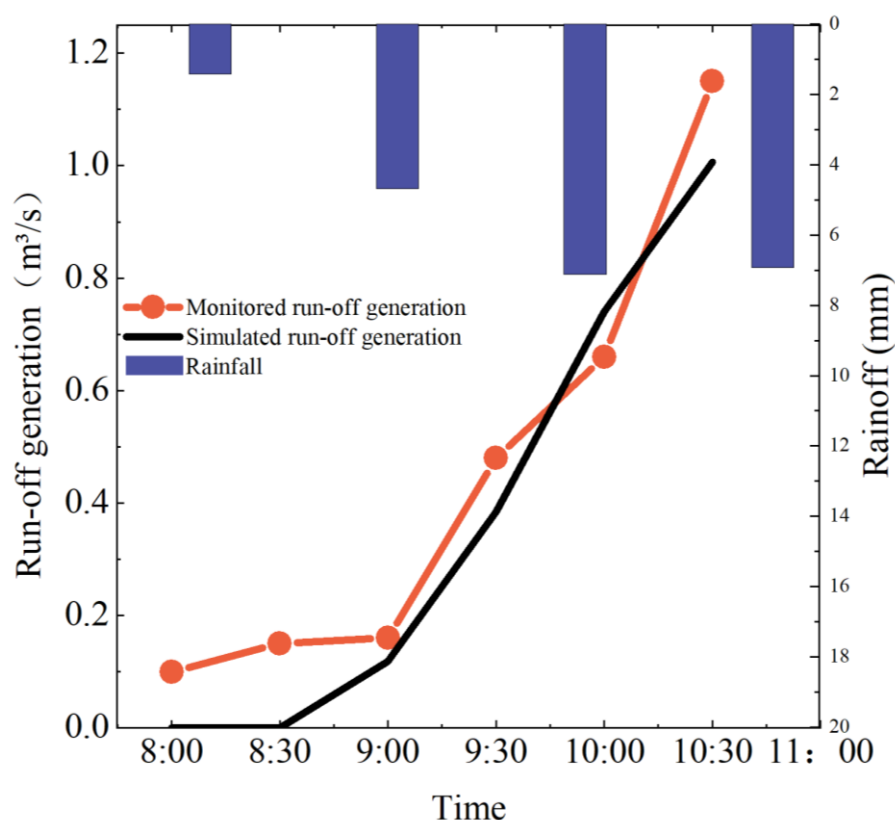


Figure 3. Checking chart on 12 July 2021.

2.5. LID Layout in the SWMM Model

2.5.1. LID Selection

The application of LID facilities can effectively reduce runoff volumes and delay peak flows [31,32]. In combination, three LID facilities—bioretention ponds, rain gardens, and sunken green spaces—were selected for optimization in this study. Individual LID facilities often have multiple functions, such as bioretention ponds that can detain stormwater before it is discharged downstream, reducing peak flows and improving runoff water quality performance [33]. Rain gardens play an important role in reducing the volume and flow of stormwater and removing pollutants from urban runoff [34], while sunken green spaces provide good water retention [35]. Due to the cost and topographical constraints of shallow mountainous areas, the area and depth of the LID facilities deployed in each sub-catchment were limited, so different specifications were set for each LID facility. Additionally, considering the geological characteristics of shallow mountainous areas, the average thickness of the soil layer was 2.1 m, so the deepest depth of the LID facilities was 2 m. The depth and unit cost corresponding to the specification of each LID facility are shown in Table 2. The other parameter design values were determined according to the SWMM user manual and related literature [36].

Table 2. Table of LID facility parameters.

| Serial Number | LID Facility Types | Specification | Depth (m) | Unit Price (m ² /CNY) |
|---------------|--------------------|---------------|-----------|----------------------------------|
| A | Sunken green space | A1 | 0.1 | 11.2314 |
| | | A2 | 0.15 | 11.74095 |
| | | A3 | 0.2 | 12.2505 |
| B | Bioretention pond | B1 | 0.2 | 46.9518 |
| | | B2 | 0.25 | 47.46135 |
| | | B3 | 0.3 | 47.9709 |
| C | Rain garden | C1 | 0.4 | 93.4627 |
| | | C2 | 0.5 | 94.4818 |
| | | C3 | 0.6 | 95.5009 |
| | | C4 | 0.7 | 96.52 |
| | | C5 | 1 | 99.5773 |
| | | C6 | 2 | 109.7683 |

2.5.2. SWMM Model Construction

According to the design scope of the site, the site was divided into two major catchment zones, namely, the catchment area outside the design scope and the catchment area within the design scope. There were 28 sub-catchment zones outside the design area and 53 sub-catchment zones within it, as summarized in Figure 4. Based on the topographic characteristics of the shallow mountainous area of the study site and the actual construction plan of the project, the elevation of the site was lowered from northwest to southeast, and the LID facilities were laid out in the direction of the catchment, with three LID types and 12 specifications laid out in the sub-catchment areas within the design area.

As per the initial scheme of the layout shown in Figure 5, sunken green space was placed mainly on the northwest side of the site, in the transition zone between the Qiyun Mountains and the site, rain gardens were placed in the current lake and surrounding area of the site, and bioretention ponds were set between the sunken green space and the rain gardens. The arrangement of the LID facilities follows the topography of the site from northwest to southeast in a pattern of sunken green space—bioretention ponds—rain gardens. There were 55 catchment areas within the design area—21 sunken green spaces, 15 bioretention ponds, and 19 rain gardens—and the initial LID facility area scheme was set at 0. The parameters of the various LID facilities are shown in the supplementary documentation (Table S1).

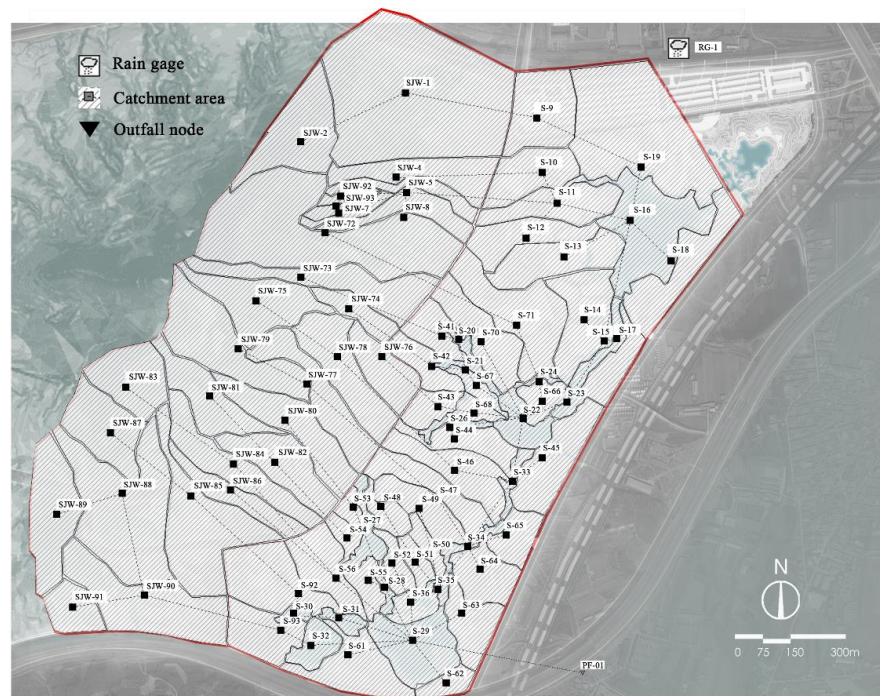


Figure 4. An SWMM overview map of the study area.

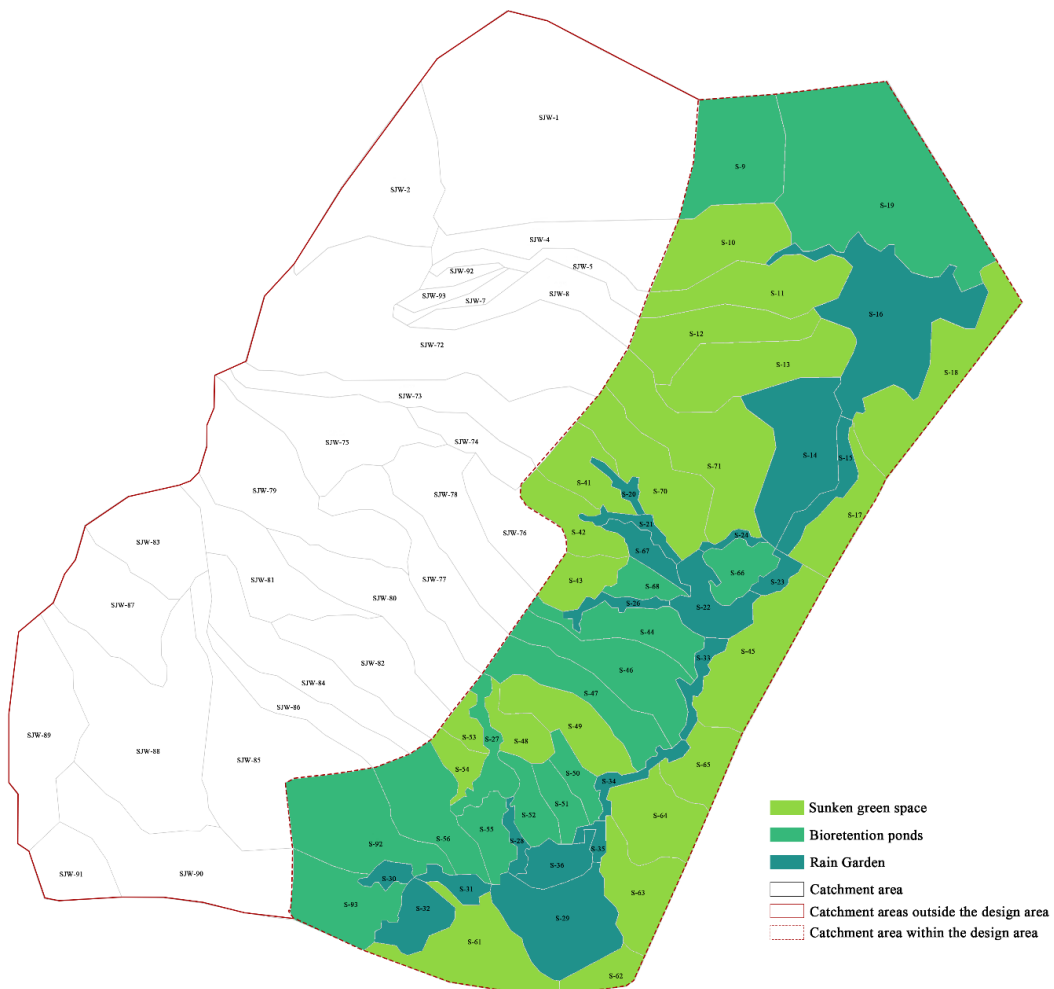


Figure 5. Initial scheme of the LID facility layout.

2.6. Genetic Algorithms

The optimization of LID facilities is fraught with complexity and involves multi-objective optimization. However, among the multi-objective optimization algorithms, the intelligent optimization algorithm non-dominated ranking genetic algorithm (NSGA-II) is one of the more commonly used, particularly for flood management and reservoir calls [37,38].

2.6.1. Selection of Optimization Targets

The construction objectives of a sponge city include peak flow control, total stormwater runoff, and pollutant control [39]. As the study site is prone to flooding in the summer and according to the “Technical Guide for Sponge City Construction,” the peak runoff abatement rate was selected as the objective function of the rainfall control effect [24], while considering that the nature of the site belongs to shallow mountainous and limited construction areas, the LID facility deployment area and cost were selected as the objective. The following are the three objective functions:

(1) Peak runoff reduction rate

Based on the storm intensity equation, a short ephemeral storm event with a 30-year return period was designed to simulate and analyze the peak runoff abatement rate of the hydrological model with and without an LID facility.

$$F_1 = \frac{\text{Runoff}_{\text{withoutLID}} - \text{Runoff}_{\text{withLID}}}{\text{Runoff}_{\text{withoutLID}}} \cdot 100\% \quad (4)$$

In Equation (4), F_1 represents the peak runoff abatement rate, $\text{Runoff}_{\text{withoutLID}}$ represents the peak flow without LIDs, and $\text{Runoff}_{\text{withLID}}$ represents the peak flow with LIDs.

(2) Construction cost

The construction cost of the LID facilities was calculated according to the construction specifications and concerning the specified design parameters of said LID facilities. The construction costs of LID facilities of different specifications are shown in Table 2.

$$F_2 = \sum_{i=1}^{55} \text{COST}_i \quad (5)$$

$$\text{COST}_i = S_i^j \cdot \text{Lcc}_i^j \quad (6)$$

In Equation (5), F_2 is the total construction cost of an LID and COST_i is the construction cost of an LID facility in sub-catchment i . In Equation (6), S_i^j is the area of facility type j in sub-catchment i and Lcc_i^j is the unit cost of facility type j in sub-catchment i .

(3) LID area

The total area of the LID facilities was the third indicator function for determining the optimal layout of the LIDs.

$$F_3 = \sum_{i=1}^{55} \text{AREA}_i \quad (7)$$

In Equation (7), F_3 represents the total built-up area of the LID and AREA_i is the area of the LID facility in sub-catchment i .

2.6.2. Constraints

(1) For the LID area objective function, we set the following constraints:

$$0 \leq S_i^j \leq S_i \quad (8)$$

In Equation (8), S_i^j denotes the area of class j facilities in sub-catchment i and S_i denotes the area of sub-catchment i .

- (2) For the construction standard of a sponge city, the optimized results of the genetic algorithm should meet the urban flooding drainage standard of the city to which the study site belongs. According to Equation (2), the total storage volume of the study site should be greater than or equal to 156,322.82 m³, and the constraint function on the total storage of the site was constructed as follows:

$$T = \sum_{i=1}^{55} TXL_i \quad (9)$$

$$TXL_i = S_i^j \cdot h_i^j \quad (10)$$

$$T \geq 156322.82$$

In Equation (9), T represents the total storage volume and TXL_i denotes the storage volume of sub-catchment i . In Equation (10), S_i^j denotes the area of facility type j in sub-catchment i and h_i^j denotes the depth of facility type j in sub-catchment i .

2.6.3. Determining the Optimization Scheme

To comprehensively evaluate the impact of the three indicators on the LID optimization scheme, a general objective function “ F ” was set. “ F ” is a multi-objective optimization general objective function on the peak runoff reduction rate, cost, and LID facility area, and the evaluation criterion of this objective function is: the larger the peak runoff reduction rate, the smaller the cost and LID facility area and the better the scheme. The objective function considering the peak runoff reduction rate–cost–area is shown in Equation (11).

$$F = \begin{cases} F_{3\min} = \sum_{i=1}^{55} Area_i \\ F_{2\min} = \sum_{i=1}^{55} COST_i \\ F_{1\max} = \frac{Runoff_{withoutLID} - Runoff_{withLID}}{Runoff_{withoutLID}} \cdot 100\% \end{cases} \quad (11)$$

2.6.4. Genetic Algorithm Optimization Process

The operation of genetic algorithms consists of three main steps: selection, crossover, and mutation [40]. As Qinhuangdao city uses a 30-year storm design as the standard for sponge city construction, the runoff process generated by a 30-year storm with a rainfall duration of three hours was selected as the base flow in the study area. Three objective functions and constraints were then written, and the initial population size was set to 50 with 200 iterations, considering that the results were only to be used for comparison with the post-construction scenario. The area parameters for a total of 12 LID facilities in three categories were simulated to filter out the optimal solution (Figure 6). The optimal solution was obtained for the lowest LID construction cost and the smallest LID installation area for different runoff peak abatement rate control objectives.

2.7. TOPSIS Analysis Method for Evaluating Solutions

The TOPSIS method is a widely used ranking method in multi-objective decision analysis, where solutions are ranked by calculating their distance from the optimal and worst solutions [41,42]. The TOPSIS method follows the following five steps: Normalization of the data matrix (Equation (12)), definition of target weights, calculation of positive and negative ideal solutions (Equations (13) and (14)), calculation of the similarity of each solution with the optimal solution (Equation (15)), and ranking according to similarity [42].

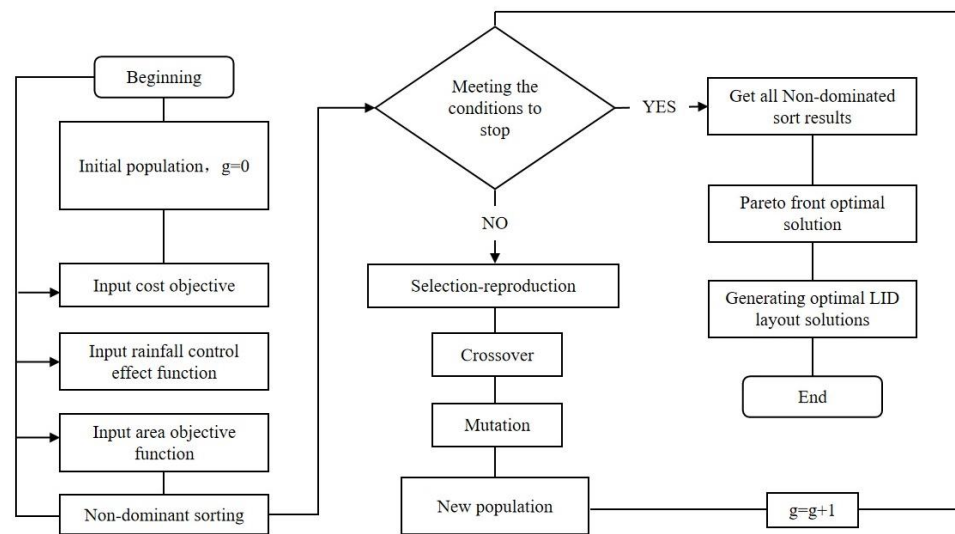


Figure 6. Genetic algorithm optimization flow chart.

$$r_{ij} = \frac{x_{ij}}{\sqrt{\sum_{k=1}^m x_{kj}^2}} \quad i = 1, 2, \dots, m \quad j = 1, 2, \dots, n \quad (12)$$

where r_{ij} denotes the normalized evaluation matrix and x_{ij} is the original evaluation matrix with i alternatives and j criteria.

$$d_i^+ = \sqrt{\sum_{j=1}^n \left((v_{ij} - v_j^+) \cdot w_j \right)^2}, \quad i = 1, 2, \dots, m \quad (13)$$

$$d_i^- = \sqrt{\sum_{j=1}^n \left((v_{ij} - v_j^-) \cdot w_j \right)^2}, \quad i = 1, 2, \dots, m \quad (14)$$

where d^+ denotes the distance between the target alternative and the best alternative, d^- denotes the distance between the target alternative and the worst alternative, and the best alternative v^+ and the worst alternative v^- contain the best and worst values for each criterion, respectively; w_j is the weight of the j th criterion.

$$cl_i = \frac{d_i^-}{d_i^- + d_i^+} \quad (15)$$

where cl_i indicates how similar the target solution is to the best solution; the higher the similarity, the more desirable the solution.

However, the uncertainty of decision makers' preferences in the decision of schemes will lead to different final election results [43]. Therefore, we can define the weights of different goals to further study the changes in the generated schemes under different weights to provide more options for decision makers. On this basis, two weighting methods were used. The first 100 generated base solutions were calculated using an objective assignment method, namely, the entropy weighting method (EWM), which calculates the weighting percentage of the three objectives. As explained by the basic principles of information theory, the more dispersed the data, the lower the entropy value, and the more information that can be artificially contained, the greater the weighting. In this case, ranking was performed and the best and worst solutions were selected. The weights generated in this case are unique and the formula for calculating weights by the entropy method is as follows:

$$\begin{aligned}
 w_j &= (1 - e_j) / \sum_{j=1}^n (1 - e_j) \\
 e_j &= \frac{-1}{\ln(m)} \sum_{i=1}^m p_{ij} \ln(p_{ij}) \\
 p_{ij} &= r_{ij} / \sum_{i=1}^r r_{ij}
 \end{aligned}
 \tag{16}$$

where w_j denotes the weight of each indicator, e_j denotes the entropy value of the j th indicator, and p_{ij} denotes the weight of the i th sample value under the j th indicator about that indicator.

Therefore, the variable area weighting method was introduced [44], defining the construction area with weights between [0.05, 0.95], and the remaining weights of peak runoff abatement rate and construction cost were equally divided to explore the changes in the similarity of the construction area for 100 scenarios with different weighting constraints

3. Results and Discussion

3.1. Analysis of the Genetic Algorithm Optimization Results

Rainwater control for the study area was based on a multi-objective optimized LID layout, coupled with the SWMM model and the NSGA-II algorithm, with the objectives of maximum peak runoff abatement rate and minimum construction cost and construction area. The land use area and storage volume were used as constraints to optimize different types of LID layout schemes, ultimately generating a total of 20,000 general solutions and 100 optimal solutions, as illustrated in Figure 7. The green legend is the general solution and the red legend is the optimal solution.

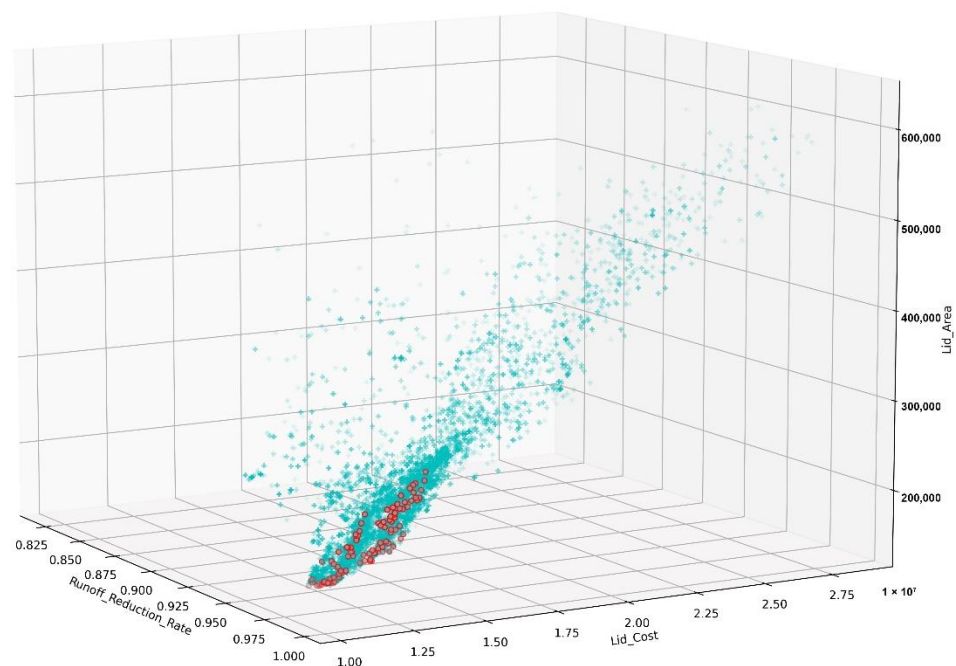


Figure 7. Genetic algorithm optimization results.

3.1.1. Peak Runoff Abatement Rate–Cost Analysis

Figure 8 shows the Pareto curve generated after the optimal solution was screened using NSGA-II optimization. It also shows the relationship between the peak runoff abatement rate and cost, which is a positive correlation. Each point in the graph represents an LID layout solution, and as shown, the peak runoff abatement rate varied from 97.9% to 99.6%, with the corresponding cost variation ranging from CNY 1.06 to 1.36 million.

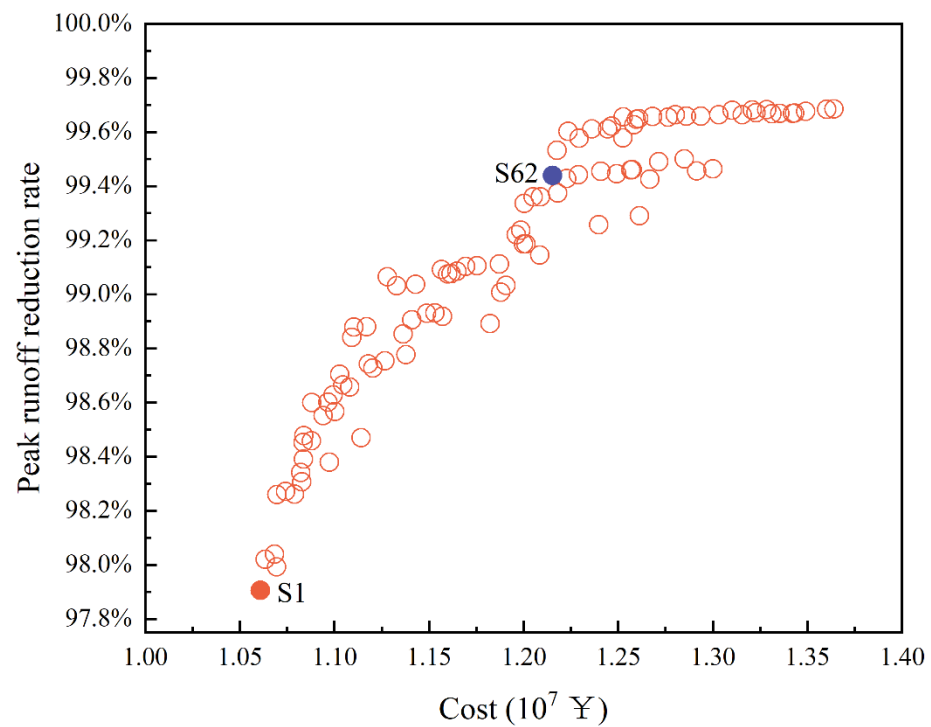


Figure 8. A plot of the peak runoff abatement rate–cost relationship.

Table 3 shows the area and cost of the LID scenarios for different peak runoff abatement rates, which were selected from the Pareto optimal solution. When the peak runoff abatement rate target was set at $98 \pm 0.2\%$, the optimal scenario was S1 and the lowest cost was CNY 10,609,939, with a peak runoff abatement rate of 97.9%. In addition, when the peak runoff abatement rate target was set at $99.6 \pm 0.2\%$, the corresponding lowest cost option was S62 with a cost of CNY 12,153,121.3. The peak runoff abatement rate was 99.43%.

Table 3. Analysis of different optimization options based on peak runoff abatement rates–cost.

| Program | S1 | S2 | S3 | S62 | S75 |
|--|--------|--------|--------|--------|--------|
| Peak runoff abatement rate | 97.90% | 97.97% | 98.02% | 99.43% | 99.6% |
| Sunken green space (km ²) | 0.04 | 0.043 | 0.049 | 0.089 | 0.089 |
| Bioretention ponds (km ²) | 0.024 | 0.025 | 0.022 | 0.048 | 0.049 |
| Rainwater garden (km ²) | 0.084 | 0.084 | 0.084 | 0.083 | 0.084 |
| Total construction area (km ²) | 0.148 | 0.152 | 0.155 | 0.22 | 0.222 |
| Percentage of LID facilities | 12.54% | 12.79% | 12.82% | 15.49% | 15.48% |
| Total construction cost (CNY 10 ⁷) | 1.061 | 1.069 | 1.063 | 1.215 | 1.223 |

3.1.2. Peak Runoff Abatement Rate–Area Analysis

The shallow mountainous terrain resulted in a limited area for the deployment of LID facilities, and therefore, the area of LID facilities is also a consideration for decision makers. Figure 9 shows that there was a positive correlation between the peak runoff abatement rate and LID area, with a higher peak runoff abatement rate resulting in a requirement for more LID facilities. As shown in the figure, the peak runoff abatement rate varied from 97.9% to 99.6% and the corresponding area varied from 0.148 to 0.271 km².

Table 4 shows the area and cost of the LID program for different peak runoff abatement rates, selected from the Pareto optimal solution. When the peak runoff reduction rate target was set at $98 \pm 0.2\%$, the corresponding LID scheme was S1, with a minimum area of 0.1486 km², as well as 0.04 km² of sunken green space, 0.024 km² of bioretention ponds, and 0.084 km² of rain gardens. When the peak runoff abatement rate target was set at

99.6 ± 0.2%, the minimum area option was S60, with 0.051 km² of sunken green space, 0.05 km² of bioretention ponds, and 0.092 km² of rain gardens, for a total construction area of 0.193 km².

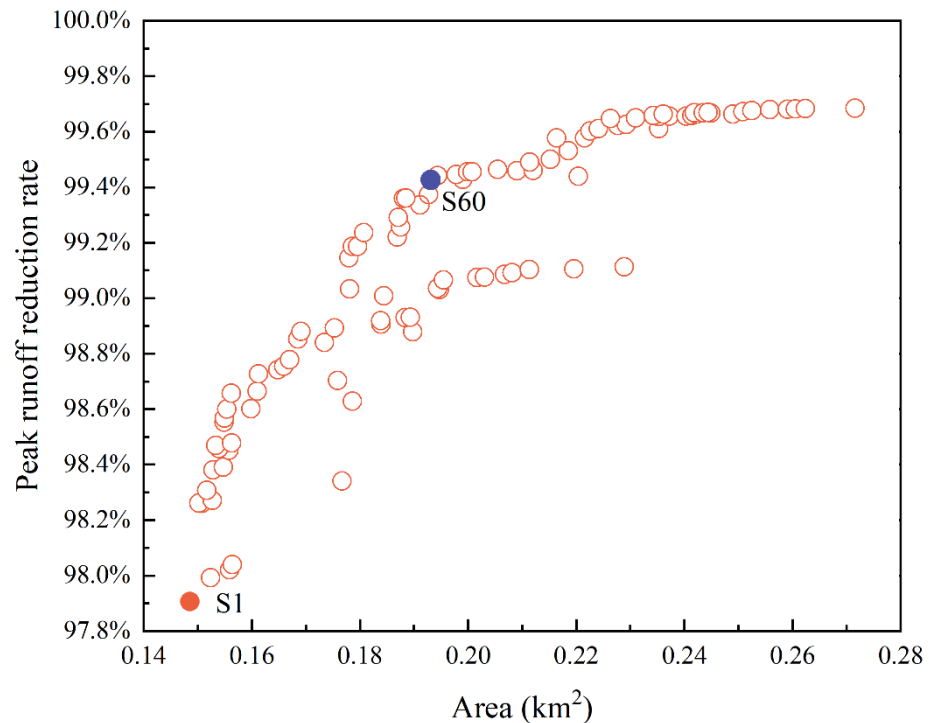


Figure 9. A plot of the peak runoff abatement rate–area relationship.

Table 4. Analysis of different optimization options based on peak runoff abatement rate–area.

| Program | S1 | S3 | S60 | S71 | S75 |
|--|--------|--------|--------|--------|--------|
| Peak runoff abatement rate | 97.90% | 98.00% | 99.42% | 99.5% | 99.6% |
| Sunken green space | 0.04 | 0.049 | 0.051 | 0.072 | 0.089 |
| Bioretention ponds | 0.024 | 0.023 | 0.05 | 0.053 | 0.049 |
| Rainwater garden | 0.084 | 0.084 | 0.092 | 0.090 | 0.084 |
| Percentage of LID facilities | 12.54% | 12.82% | 15.25% | 15.43% | 15.48% |
| Total construction area (km ²) | 0.148 | 0.156 | 0.193 | 0.215 | 0.222 |
| Total construction cost (CNY 10 ⁷) | 1.061 | 1.063 | 1.267 | 1.285 | 1.223 |

3.2. Analysis of The Results Based on the EWM-TOPSIS and VCWM-TOPSIS Methods

As the study site is a shallow mountainous area, the construction area was considered to have a large influence on the decision. Therefore, the weight vectors for the three objectives (peak runoff abatement rate, construction cost, and construction area) were [0.008, 0.154, 0.8452], respectively, using the entropy weighting method. It can be seen that area was the most important criterion. The results for the peak runoff abatement rate fluctuated between 97.9% and 99.6%, with little dispersion, so the result with the lowest weight is reasonable. The relative proximity values were obtained by performing a ranking calculation using TOPSIS analysis. Figure 10 shows the similarity curves of the 100 best solutions, where the best solution was S80, with a similarity of 87%, a peak runoff abatement rate of 99.65%, a construction area of 0.226 km², and a cost of CNY 12,595,149.74. Meanwhile, the worst solution was S1, with a similarity of 16%, a peak runoff abatement rate of 97.91%, a construction area of 0.148 km², and a cost of CNY 10,609,939.69.

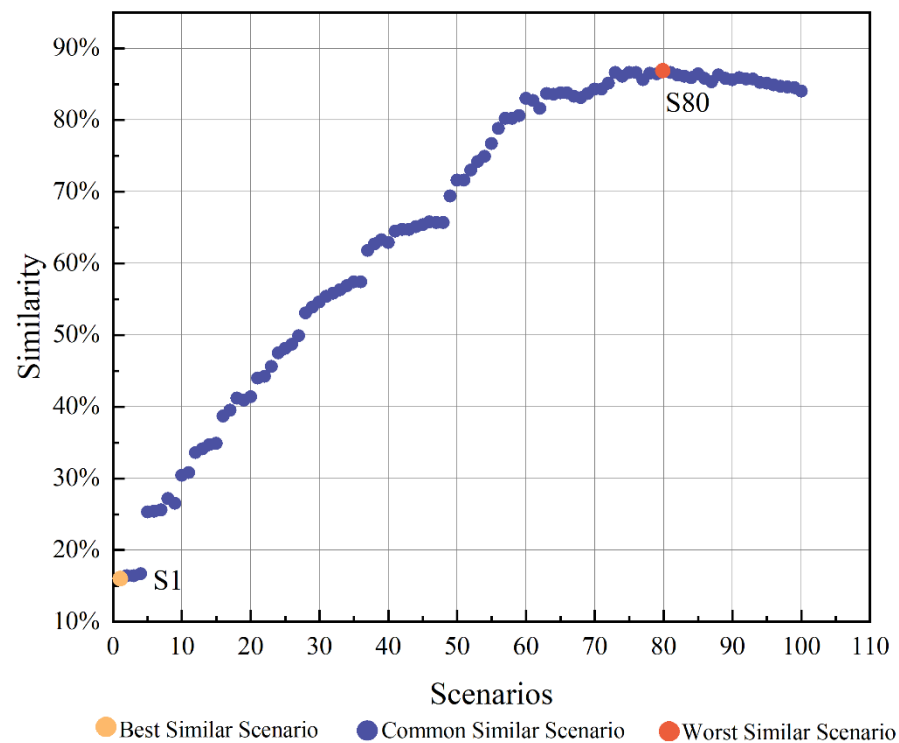


Figure 10. The similarity of 100 scenes by the EWM-TOPSIS method.

In addition to this, the weighting of the built-up area was further investigated in this paper to explore the layout pattern of LID facilities in shallow mountainous areas. The EWM-TOPSIS method of analysis yields the weight of the construction area accounting for the largest proportion; thus, further exploring the effect of when the weight of the built-up area is in an interval of variation on the selection of the final result. Based on this, using the variable area weighting method (VCWM), Figure 11 illustrates the change in the similarity of the 100 optimal solutions under the influence of changing area weights. Based on the similarity curves, the 100 layout solutions can be classified into two types, i.e., benefit and cost. As the area weight increased, the similarity of the benefit-type curve increased while that of the cost-type curve decreased. The similarity curves with similarity intervals between [0.8, 1] were selected for in-depth analysis. When the area weights were between [0.3, 0.45], the benefit type gradually replaced the cost type. This indicates that the cost-based solution is more desirable under a low weight constraint, while the benefit-based solution is desirable under a high weight constraint. In the overall analysis, the trend of the similarity curves for the 100 scenarios changed significantly for weight change values between [0, 0.45], while the similarity curves for [0.45, 1] tended to flatten out. This suggests that area weights have a greater impact on decision outcomes under low constraints and that decision makers encounter more complexity in choosing a final scenario in this weight range. This implies that building in shallow mountainous areas should be more concerned with the fineness of the area weights; otherwise, it is difficult to balance the relationship between construction effectiveness and area.

3.3. Comparison of Optimal Solutions

The genetic algorithm optimization of the optimal solutions S62 and S60 based on cost and area preference, respectively, and the optimal solution S80 after EWM-TOPSIS ranking were compared to the actual construction solution. The cost and area of the actual construction option were derived from the comprehensive project estimate table and were $\text{CNY } 2.54 \times 10^7$ and 0.20 km^2 , respectively. The peak runoff abatement rate was compared to the option without LID facilities, and the peak runoff abatement rate of the actual option was 100%, which is reasonable, as the pre-designed purpose at the beginning was to abate

the runoff from the entire Qiyun Mountains and surrounding roads and urban areas. The comparison results are shown in Table 5. The construction cost of S62, S60, and S80 was less than the actual construction side, and the construction area was lower than the actual construction solution in the area-based preference solution S60. Therefore, the genetic algorithm-optimized program under the performance of different preferences was better than the actual construction project.

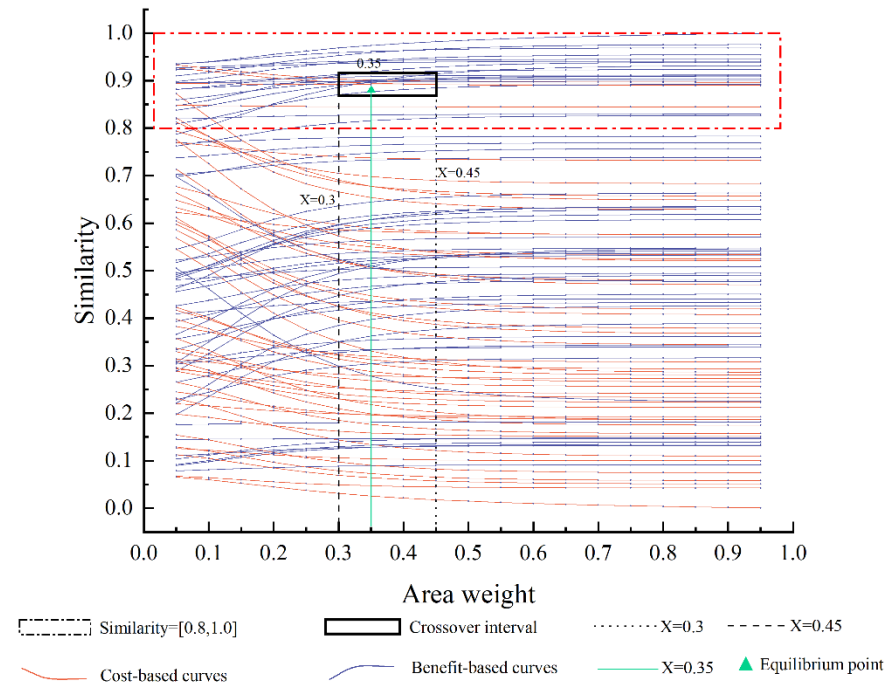


Figure 11. Similarity curves for 100 scenes by the variable weight-TOPSIS method.

Table 5. Comparison of the optimal solutions.

| Scenarios | S62 | S60 | S80 | Actual Construction Program |
|--|--------|--------|--------|-----------------------------|
| Peak runoff abatement rate | 99.43% | 99.42% | 99.65% | 100% |
| Total construction area (km ²) | 0.22 | 0.193 | 0.226 | 0.20 |
| Total construction cost (CNY 10 ⁷) | 1.215 | 1.267 | 1.256 | 2.54 |

4. Conclusions

In this study, we used NSGA-II coupled with SWMM to find the optimal LID layout scheme based on a multi-objective combination of peak runoff abatement rate, construction cost, and construction area. One hundred non-dominated solutions were generated after 20,000 calls to the SWMM by NSGA-II, which constituted the Pareto front. The three objective weights were determined by two methods, and the 100 solutions were ranked using the TOPSIS method to find the best of the 100 solutions and the impact of area performance on the final decision.

The model was enhanced by collecting actual monitoring data to validate the model and greatly improve the simulation accuracy. The algorithm-generated solutions were also compared to the actual construction solutions to further verify whether the decision solutions made by the algorithm under preference guidance are better than those generated by the subjective judgement of decision makers.

The main findings are as follows:

1. Through the analysis of 100 non-dominated solutions, the peak runoff abatement rate and construction cost and construction area were positively correlated. When the area was prioritized, the LID facilities accounted for 15.25% and the peak runoff abatement

- rate was 99.42%, and when the LID costs were prioritized, the LID facilities accounted for 15.49% and the peak runoff abatement rate was 99.43%.
2. The EWM-TOPSIS method ranked the best solution as S80, with a construction area share of 16.18%, a peak runoff abatement rate of 99.64%, and a cost of CNY 12,595,149.74. The worst solution was S1, with a construction area share of 12.54%, a peak runoff abatement rate of 97.90%, and a cost of CNY 10,609,939.69.
 3. Using the TOPSIS method with variable weights, based on the change in similar curves with weights into two categories, with the change in weights, the two types of curves reached an equilibrium point. When the equilibrium point fluctuated in the interval [0, 0.3], the area was under low constraint. In the actual construction project, this means that in a gentler site for sponge city construction, the cost-based scheme is preferable. Meanwhile, a [0.3, 0.6] fluctuation indicates that the area is under high constraint, meaning that sites with larger topographic slopes are more suitable for the benefit-based option. The changing weighting of area performance and the emergence of equilibrium points are relevant in actual projects.
 4. By making a comparison with the built scheme, the case study of the Qinhuangdao City Garden Flower Expo Park shows that when optimizing the LID layout at the shallow mountain level, from the aspect of land intensification, genetic algorithms combined with various hydrological models and multi-objective optimization are effective for decision making on LID facilities. Meanwhile, the final generated results using TOPSIS ranking can effectively control construction intensity based on decision makers' preferences, save investment, achieve large peak runoff abatement rates, and efficiently build a region-wide sponge city system.
 5. In addition, there are a number of limitations to this paper. Although water quality was sampled during the monitoring process, only COD pollutants were used and sampling for other pollutants was lacking; therefore, indices of water quality were not considered in this study. Further water quality indices could be incorporated into multi-objective optimization at a later stage.

Supplementary Materials: The following supporting information can be downloaded at: <https://www.mdpi.com/article/10.3390/w14192986/s1>, Table S1: The parameter values required by LID control Module in SWMM.

Author Contributions: Conceptualization, H.S. and X.G.; Investigation, X.L.; Methodology, H.S. and Y.D.; Software, Y.D. and C.L.; Validation, H.S., Y.L. and X.L.; Formal analysis, H.S. and Y.D.; Writing—original draft preparation, H.S.; Writing—review and editing, H.S., Y.D. and X.G.; Visualization, H.S. and Y.D.; Supervision, X.G.; Project management, X.G.; Funding acquisition, X.G.; H.S. and Y.D. contributed to the work equally and should be regarded as co-first authors. X.G. and C.L. should be regarded as co-correspondence. All authors have read and agreed to the published version of the manuscript.

Funding: This research was funded by the Fundamental Research Funds for the Central Universities (grant number NO. 2021ZY38), the National Natural Science Foundation of China (grant number 31800606), Beijing Social Science Foundation (grant number 21JCC094), Beijing Scientific Research and Postgraduate Education Jointly Construction (grant number 2015BLUREE01).

Institutional Review Board Statement: Not applicable.

Informed Consent Statement: Not applicable.

Data Availability Statement: Data sharing is not applicable to this article.

Acknowledgments: The authors are grateful for the anonymous reviewers' careful review and constructive suggestions to improve the manuscript.

Conflicts of Interest: The authors declare no conflict of interest.

References

1. Wang, K. Research and Discussion on the Current Situation and Problems of Sponge City Construction. *Value Eng.* **2022**, *41*, 11–13.
2. Huang, L. Study on Systematic and Global Measures to Promote the Construction of Sponge City. *Jiangxi Build. Mater.* **2022**, *42*, 269–270.
3. Ministry of Housing and Urban-Rural Development of the People's Republic of China. Available online: https://www.mohurd.gov.cn/xinwen/gzdt/202204/20220415_765693.html (accessed on 18 August 2022).
4. Chen, H. *Research on the Planning and Design of Forest-Wetland Park in Foothill Area in Beijing from the Perspective of Rainwater Management—A Case Study of Miyun Forest-Wetland Park*; Beijing Forestry University: Beijing, China, 2020.
5. Liu, F.; Cheng, W.; Liu, X.; Jia, R.; Du, C.; Wang, M. Research Progress and Application of Low impact Development in Sponge City Construction. *Water Purif. Technol.* **2022**, *41*, 1–7.
6. Saadatpour, M.; Delkosh, F.; Afshar, A.; Solis, S.S. Developing a simulation-optimization approach to allocate low impact development practices for managing hydrological alterations in urban watershed. *Sustain. Cities Soc.* **2020**, *61*, 102334. [[CrossRef](#)]
7. Dong, F.; Zhang, Z.; Liu, C.; Zou, R.; Liu, Y.; Guo, H. Towards efficient Low Impact Development: A multi-scale simulation-optimization approach for nutrient removal at the urban watershed. *J. Clean. Prod.* **2020**, *269*, 122295. [[CrossRef](#)]
8. Sun, H.; Bian, R.; Li, R.; Cao, X.; Qi, W.; Peng, J.; Li, S.; He, X.; He, X. Evaluation of best management practices (BMPs) for phosphorus load reduction based on SWAT model. *Acta Sci. Circumstantiae* **2020**, *40*, 403–412.
9. Kang, H. *Research on Non-Point Source Pollution Management Measures of Danjiang River Basin Based OnSWAT Model*; Xi'an University of Technology: Xi'an, China, 2020.
10. Xu, T.; Jia, H.; Wang, Z.; Mao, X.; Xu, C. SWMM-based methodology for block-scale LID-BMPs planning based on site-scale multi-objective optimization: A case study in Tianjin. *Front. Environ. Sci. Eng.* **2017**, *11*, 1. [[CrossRef](#)]
11. Tang, S.; Jiang, J.; Shamseldin, A.Y.; Shi, H.; Wang, X.; Shang, F.; Wang, S.; Zheng, Y. Comprehensive Optimization Framework for Low Impact Development Facility Layout Design with Cost-Benefit Analysis: A Case Study in Shenzhen City, China. *ACS EST Water* **2022**, *2*, 63–74. [[CrossRef](#)]
12. Giacomoni, M.H.; Joseph, J. Multi-Objective Evolutionary Optimization and Monte Carlo Simulation for Placement of Low Impact Development in the Catchment Scale. *J. Water Resour. Plan. Manag.* **2017**, *143*, 04017053. [[CrossRef](#)]
13. Hou, J.; Yuan, H. Optimal spatial layout of low-impact development practices based on SUSTAIN and NSGA-II. *Desalination Water Treat.* **2020**, *177*, 227–235. [[CrossRef](#)]
14. Huang, J.J.; Xiao, M.; Li, Y.; Yan, R.; Zhang, Q.; Sun, Y.; Zhao, T. The optimization of Low Impact Development placement considering life cycle cost using Genetic Algorithm. *J. Environ. Manag.* **2022**, *309*, 114700. [[CrossRef](#)] [[PubMed](#)]
15. Liu, Z.; Xu, C.; Xu, T.; Jia, H.; Zhang, X.; Chen, Z.; Yin, D. Integrating socioecological indexes in multiobjective intelligent optimization of green-grey coupled infrastructures. *Resour. Conserv. Recycl.* **2021**, *174*, 105801. [[CrossRef](#)]
16. He, L.; Li, S.; Cui, C.H.; Yang, S.S.; Ding, J.; Wang, G.Y.; Bai, S.W.; Zhao, L.; Cao, G.L.; Ren, N.Q. Runoff control simulation and comprehensive benefit evaluation of low-impact development strategies in a typical cold climate area. *Environ. Res.* **2022**, *206*, 112630. [[CrossRef](#)]
17. Wang, D.; Fu, X.; Luan, Q.; Liu, J.; Wang, H.; Zhang, S. Effectiveness assessment of urban waterlogging mitigation for low impact development in semi-mountainous regions under different storm conditions. *Hydrol. Res.* **2021**, *52*, 284–304. [[CrossRef](#)]
18. Liu, B.; Peng, J.; Zhang, J.; Liu, J.; Wang, C.; Xie, Z.; Chen, P.; Wang, H.; Yue, J.; Hui, X.; et al. *Hebei Province Public Policy Assessment Blue Book—2018 Business Environment Assessment of Qinhuangdao, etc.*; Yanshan University Press: Qinhuangdao, China, 2019; pp. 119–146.
19. Lu, Y.; Ge, X. Method for Designing Urban Green Space Water System Based on Water Security: A Case Study of 2nd Hebei Garden Expo (Qinhuangdao) Park. *Landsc. Archit.* **2020**, *27*, 64–69.
20. Sun, L.; Qi, Y.; Zhang, B.; Wu, J. The Characteristics of Natural Rainfall in Recent 63 Years in Qinhuangdao. *J. Hebei Univ. Environ. Eng.* **2017**, *27*, 35–38.
21. University, H.A. *Engineering Technical Specification for Construction of the Sponge City*; Department of Housing & Urban-Rural Development Hebei: Shijiazhuang, China, 2016; p. 46.
22. Shanghai Municipal Commission of Housing and Urban-rural Development. *Standard for Design of Outdoor Wastewater Engineering*; Ministry of Housing and Urban-Rural Development of the People's Republic of China: Shanghai, China, 2021; pp. 11–12.
23. Ministry of Housing and Urban-Rural Development of the People's Republic of China. *Technical Code for Urban Flooding Prevention and Control*; China Planning Press: Shanghai, China, 2017; pp. 7–11.
24. Ministry of Housing and Urban-Rural Development of the People's Republic of China. *Technical Guide for Sponge City Construction—Construction of Rainwater System for Low Impact Development*; Ministry of Housing and Urban-Rural Development of the People's Republic of China: Beijing, China, 2014; pp. 49–50.
25. Ministry of Housing and Urban-Rural Development of the People's Republic of China. *Planting Soil for Greening*; Standards Press of China: Beijing, China, 2016; pp. 5–6.
26. Liu, X. A Review of Research on Calibration of Urban Stormwater Network Model Parameters. *Water Wastewater Eng.* **2009**, *45*, 452–455.
27. Zhang, H. *Low Impact Development of the SpCities—The Research of the Typical Mountain Runoff Effect*; Hebei University of Engineering: Handan, China, 2016.

28. Li, D.; Ye, C.-Q. Multi-objective Optimization of Low Impact Development Using SWMM Model and NSGA-Method and Its Application. *Water Resour. Power* **2019**, *37*, 58–61.
29. Hodson, T.O. Root-mean-square error (RMSE) or mean absolute error (MAE): When to use them or not. *Geosci. Model Dev.* **2022**, *15*, 5481–5487. [[CrossRef](#)]
30. Bahrami, E.; Salarijazi, M.; Nejatian, S. Estimation of food hydrographs in the ungauged mountainous watershed with Gray synthetic unit hydrograph model. *Arab. J. Geosci.* **2022**, *15*, 761. [[CrossRef](#)]
31. Sohn, W.; Kim, J.H.; Li, M.H.; Brown, R. The influence of climate on the effectiveness of low impact development: A systematic review. *J. Environ. Manag.* **2019**, *236*, 365–379. [[CrossRef](#)] [[PubMed](#)]
32. Wang, D.; Zhang, X.; Luan, Q.; Zhang, K.; Fu, X.; Liu, J. Evaluation on application of low impact development technology in hilly zone of semi-mountainous region. *Water Resour. Hydropower Eng.* **2019**, *50*, 115–123.
33. Vijayaraghavan, K.; Biswal, B.K.; Adam, M.G.; Soh, S.H.; Tsen-Tieng, D.L.; Davis, A.P.; Chew, S.H.; Tan, P.Y.; Babovic, V.; Balasubramanian, R. Bioretention systems for stormwater management: Recent advances and future prospects. *J. Environ. Manag.* **2021**, *292*, 112766. [[CrossRef](#)] [[PubMed](#)]
34. Bak, J.; Barjenbruch, M. Benefits, Inconveniences, and Facilities of the Application of Rain Gardens in Urban Spaces from the Perspective of Climate Change—A Review. *Water* **2022**, *14*, 1153. [[CrossRef](#)]
35. Jia, L.; Xu, G.; Huang, M.; Li, Z.; Li, P.; Zhang, Z.; Wang, B.; Zhang, Y.; Zhang, J.; Cheng, Y. Effects of Sponge City Development on Soil Moisture and Water Quality in a Typical City in the Loess Plateau in China. *Front. Earth Sci.* **2020**, *8*, 125. [[CrossRef](#)]
36. Lin, C.-S.; Shao, M.; Ge, Y.-Y.; GE, X.-Y. Research of storm flood regulation efficiency of the low impact development of exogenous-rainwater park based on the SWMM simulation. *J. Beijing For. Univ.* **2016**, *38*, 92–103.
37. Pang, L.M.; Ishibuchi, H.; Shang, K. NSGA-II with Simple Modification Works Well on a Wide Variety of Many-Objective Problems. *IEEE Access* **2020**, *8*, 190240–190250. [[CrossRef](#)]
38. Chlumecký, M.; Buchtele, J.; Richta, K. Application of random number generators in genetic algorithms to improve rainfall-runoff modelling. *J. Hydrol.* **2017**, *553*, 350–355. [[CrossRef](#)]
39. Che, W.; Zhao, Y.; Li, J.-Q.; Wang, W.-L.; Wang, J.-L.; Wang, S.-S.; Gong, Y.-W. Explanation of Sponge City Development Technical Guide: Basic Concepts and Comprehensive Goals. *China Water Wastewater* **2015**, *31*, 1–5.
40. Jamshidi, M. Tools for intelligent control: Fuzzy controllers, neural networks and genetic algorithms. *Philos. Trans. R. Soc. Math. Phys. Eng. Sci.* **2003**, *361*, 1781–1808. [[CrossRef](#)] [[PubMed](#)]
41. Hwang, C.L.; Lai, Y.J.; Liu, T.Y. A new approach for multiple objective decision making. *Comput. Oper. Res.* **1993**, *20*, 889–899. [[CrossRef](#)]
42. Mirzanejad, M.; Ebrahimi, M.; Vamplew, P.; Veisi, H. An online scalarization multi-objective reinforcement learning algorithm: TOPSIS Q-learning. *Knowl. Eng. Rev.* **2022**, *37*, e7. [[CrossRef](#)]
43. Pena, J.; Nápoles, G.; Salgueiro, Y. Implicit and hybrid methods for attribute weighting in multi-attribute decision-making: A review study. *Artif. Intell. Rev.* **2021**, *54*, 3817–3847. [[CrossRef](#)]
44. Howes, D.J.; Sanders, B.F. Velocity Contour Weighting Method. I: Algorithm Development and Laboratory Testing. *J. Hydraul. Eng. Asce* **2011**, *137*, 1359–1367. [[CrossRef](#)]